

# Templated Electrosynthesis of Zinc Oxide Nanorods

Min Lai and D. Jason Riley\*

School of Chemistry, University of Bristol, Cantock's Close, Bristol BS8 1TS, United Kingdom

Received July 22, 2005. Revised Manuscript Received December 15, 2005

Electrosynthesis of zinc oxide has been performed in track etched polymer membranes to yield nanorods of defined diameter and controlled length. The electrodeposition process involves two steps: (i) electroreduction of either hydrogen peroxide or nitrate ions to alter the local pH within the pores and (ii) precipitation of the metal oxide within the pores. Synthesis at 22 °C via the reduction of hydrogen peroxide yielded polycrystalline zinc oxide nanorods. When deposition was performed at 90 °C, using the reduction of nitrate to control the local pH, zinc oxide nanorods which displayed the same growth direction along their entire length were obtained. The length of all as-grown rods increased with the integrated charge passed. The growth direction of the ZnO rods obtained at the higher temperature was unusual, being perpendicular to the (1011) plane.

## Introduction

Templated synthesis has been employed widely to prepare solids of defined dimension.<sup>1–3</sup> Several techniques of forming materials in templates have been developed, including chemical vapor deposition (CVD),<sup>4</sup> sol–gel deposition,<sup>5</sup> in situ polymerization,<sup>6</sup> and electrochemical deposition.<sup>7</sup> The latter, in which the template is adhered to an electrode surface, offers simple and precise control of the dimension of the as-formed structures, owing to the facts that (i) the material propagates, continuously through the template from the base electrode, and (ii) that the amount of solid deposited is proportional to the current passed. Direct templated electrodeposition has been employed to form nanomaterials of metals, conducting polymers, and semiconductors.<sup>8,9</sup> A variety of templates have been used in electrodeposition studies, with porous anodic aluminum oxide or nuclear track etched polymer membranes being the matrixes of choice for preparation of nanorods. In this paper, we provide a first illustration of the way in which electrochemistry can be employed to manage the pH within the pores of a template and demonstrate the controlled growth of continuous crystalline metal oxide nanorods.

ZnO is a wide band gap (3.37 eV) semiconductor with a large exciton binding energy (60 meV). One-dimensional ZnO nanostructures have been attracting intense scientific

interest as these materials exhibit near-UV emission,<sup>10</sup> UV absorption,<sup>11</sup> and field-emission capabilities.<sup>12</sup> A number of physical and chemical techniques have been developed to fabricate one-dimensional ZnO nanostructures. High-temperature thermal evaporation,<sup>13,14</sup> CVD,<sup>15,16</sup> and pulsed laser deposition<sup>17–19</sup> have been used to produce high-quality ZnO nanorods and nanowires; such procedures require rigid conditions and expensive reactors. ZnO nanorods and nanowires have also been prepared by wet chemical methods such as hydrothermal processes<sup>19–21</sup> and epitaxial electrodeposition.<sup>22</sup> Here we introduce a widely applicable and straightforward alternate strategy where ZnO nanorods of defined length can be generated by immersing an electrode coated with a track etched polymer membrane into an electrolyte containing zinc ions and then electrochemically changing the local pH; zinc oxide nanorods of defined length can be achieved. Hydrogen peroxide and nitrate ions have been employed as the electroactive species that, when reduced, result in a local pH change at the electrode interface and the precipitation of zinc oxide.

## Experimental Section

In a typical synthesis, ZnO nanorods were fabricated by electrodeposition into a nuclear track etch polycarbonate membrane

\* To whom correspondence should be addressed. E-mail: jason.riley@bristol.ac.uk. Tel.: +441179287669. Fax: +441179251295.

- Hultheen, J. C.; Martin, C. R. *J. Mater. Chem.* **1997**, *7*, 1075.
- Nicewarner-Peña, S. R.; Freeman, R. G.; Reiss, B. D.; He, L.; Peña, D. J.; Walton, I. D.; Cromer, R.; Keating, C. D.; Natan, M. J. *Science* **2001**, *294*, 137.
- Sun, L.; Searson, P. C.; Chien, C. L. *Appl. Phys. Lett.* **1999**, *74*, 2803.
- Huang, L.; Wind, S. J.; O'Brien, S. P. *Nano Lett.* **2003**, *3*, 299.
- Lakshmi, B. B.; Dorhout, P. K.; Martin, C. R. *Chem. Mater.* **1997**, *9*, 857.
- Martin, C. R.; Vandyske, L. S.; Cai, Z. H.; Liang, W. B. *J. Am. Chem. Soc.* **1990**, *112*, 8976.
- Park, S.; Lim, J. H.; Chung, S. W.; Mirkin, C. A. *Science* **2004**, *303*, 348.
- Martin, C. R. *Chem. Mater.* **1996**, *8*, 1739.
- Peña, D. J.; Mbindyo, J. K. N.; Carado, A. J.; Mallouk, T. E.; Keating, C. D.; Razavi, B.; Mayer, T. S. *J. Phys. Chem. B* **2002**, *106*, 7458.
- Service, R. E. *Science* **1997**, *276*, 895.
- Meulenkamp, E. A. *J. Phys. Chem. B* **1998**, *102*, 5566.
- Banerjee, D.; Jo, S. H.; Ren, Z. F. *Adv. Mater.* **2004**, *16*, 2028.
- Huang, M. H.; Mao, S.; Feick, H.; Yan, H. Q.; Wu, Y. Y.; Kind, H.; Weber, E.; Russo, R.; Yang, P. D. *Science* **2001**, *292*, 1897.
- Wang, X. D.; Summers, C. J.; Wang, Z. L. *Nano Lett.* **2004**, *4*, 423.
- Park, W. I.; Kim, D. H.; Jung, S. W.; Yi, G. C. *Appl. Phys. Lett.* **2002**, *80*, 4232.
- Monge, M.; Kahn, M. L.; Maisonnat, A.; Chaudret, B. *Angew. Chem., Int. Ed.* **2003**, *42*, 5321.
- Choi, J. H.; Tabata, H.; Kawai, T. *J. Cryst. Growth* **2001**, *226*, 493.
- Nobis, T.; Kaidashev, E. M.; Rahm, A.; Lorenz, M.; Lenzner, J.; Grundmann, M. *Nano Lett.* **2004**, *4*, 797.
- Sun, Y.; Fuge, G. M.; Fox, N. A.; Riley, D. J.; Ashfold, M. N. R. *Adv. Mater.* **2005**, *17*, 2477.
- Vayssieres, L. *Adv. Mater.* **2003**, *15*, 464.
- Cheng, B.; Samulski, E. T. *Chem. Commun.* **2004**, 986.
- Liu, R.; Vertegel, A. A.; Bohannan, E. W.; Sorenson, T. A.; Switzer, J. A. *Chem. Mater.* **2001**, *13*, 508.

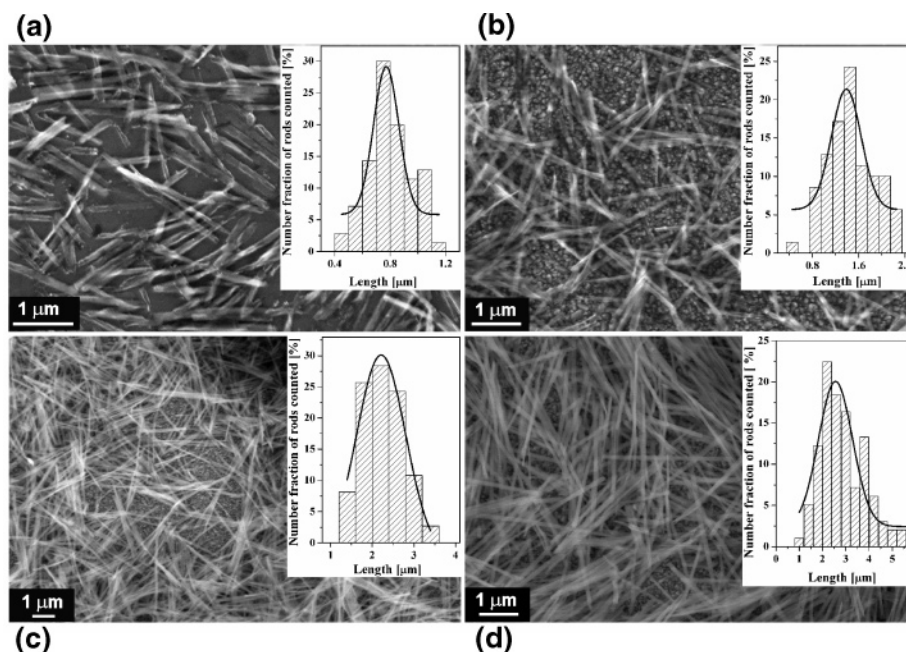


**Figure 1.** FE-SEM images of electrosynthesized ZnO nanorods prepared at 22 °C using hydrogen peroxide as the hydroxide precursor with integrated charges of (a) 0.01 C; (b) 0.02 C, (c) 0.05 C; and (d) 0.1 C. The insets show histograms of the length distribution of each sample; Gaussian fits to the data are displayed.

(Whatman, Inc.). The rated membrane thickness, nominal pore size, and pore density were respectively 6  $\mu\text{m}$ , 50 nm, and  $6 \times 10^8$  pores/ $\text{cm}^2$ . One side of the polycarbonate membrane was first coated with a 50 nm thick layer of gold, by high-vacuum evaporation, to serve as a working electrode. The electrical contact was made to the membrane working electrode using aluminum foil. A platinum mesh was used as the counter electrode, and an Ag/AgCl (3 M KCl) electrode was used as the reference electrode. Electrosynthesis was performed under potentiostatic control using an Eco Chemie  $\mu$ AUTOLAB instrument. Electrosynthesis of ZnO was performed in electrolytes containing zinc ions and either hydrogen peroxide or nitrate ions as the electrochemical hydroxide precursor. The two aqueous (Elgestat water,  $>18 \text{ M}\Omega \text{ cm}$ ) plating solutions were 5 mM  $\text{ZnSO}_4$ , 5 mM  $\text{H}_2\text{O}_2$ , and 0.1 M  $\text{Na}_2\text{SO}_4$  as the supporting electrolyte and 0.01 M  $\text{Zn}(\text{NO}_3)_2$ . The deposition when using peroxide as the precursor was performed at 22 °C at a fixed potential of  $-0.2 \text{ V}$ . Electrosynthesis in the presence of nitrate was carried out at 90 °C at a constant potential of  $-0.7 \text{ V}$ .

Following deposition the gold backing used as the working electrode was mechanically removed, and the membrane was rinsed three times in deionized water, for 10 min each time. The nanorods were released by dissolving the polycarbonate membrane in dichloromethane. The suspension was centrifuged at  $\sim 3000 \text{ rpm}$ , and the rods were washed three times with dichloromethane and finally suspended in 0.5  $\text{cm}^3$  of dichloromethane.

Samples for scanning electron microscopy (SEM) studies were prepared by drop casting the as-prepared suspension onto either indium tin oxide glass or silicon; to permit accurate determination of particle dimensions, no metal was deposited onto the as-deposited layers. SEM images were obtained using a JEOL JSM-6330FEG microscope operated at 10 kV. Transmission electron microscopy (TEM) images were recorded on a JEOL JEM-1200EX microscope operated at 120 kV. High-resolution transmission electron microscopy (HR-TEM) images were acquired on JEOL JEM-2010EX microscope at 200 kV.

## Results

### 1. Hydrogen Peroxide as the Electrochemical Source of Hydroxide Ions.

On reduction of an aqueous hydrogen

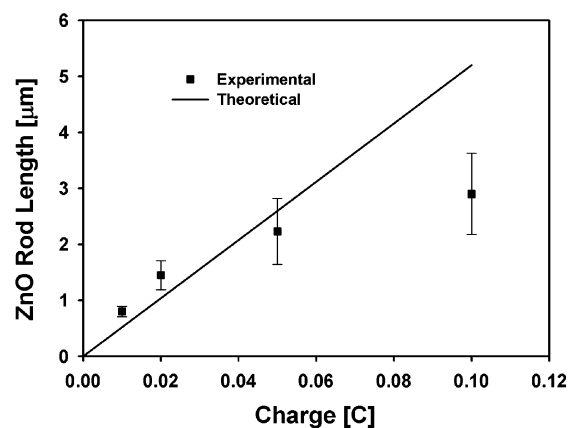


**Figure 2.** Experimental and theoretical relationships between the average length of ZnO nanorods prepared at 22 °C and integrated charge passed during electrosynthesis. The vertical bars represent the full width at half-maximum of the Gaussian fit to the size histogram. The theoretical length was calculated assuming that all hydroxide ions produced by  $\text{H}_2\text{O}_2$  reduction led to the formation of ZnO, and the nanorods have the same density as crystalline ZnO.

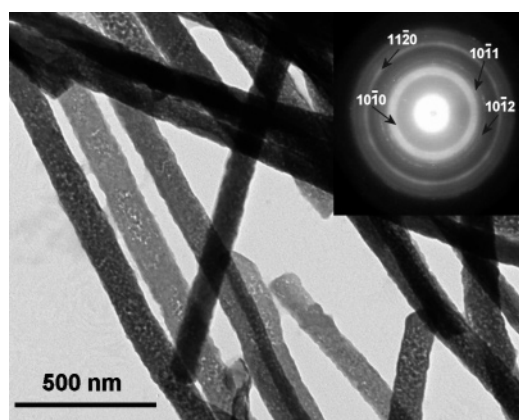


**Figure 3.** TEM image of ZnO nanorods prepared at 22 °C with an integrated charge passed of 0.1 C and the corresponding SAED pattern.

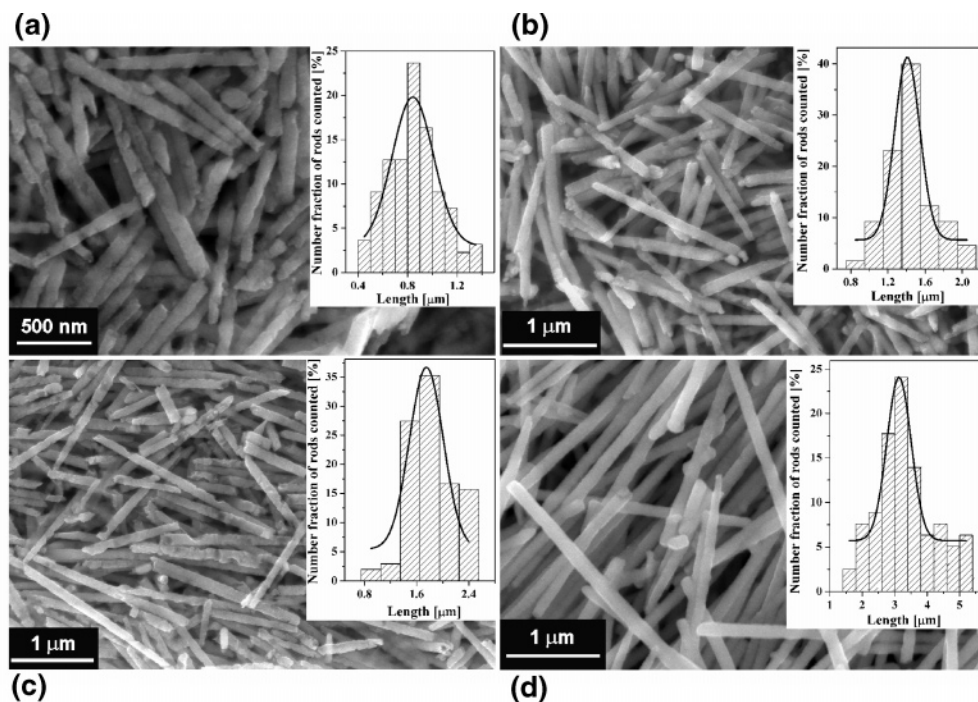
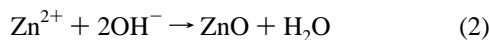
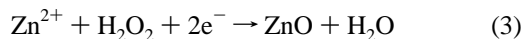


**Figure 4.** FE-SEM images of electrosynthesized ZnO nanorods prepared at 90 °C using nitrate ions as the hydroxide precursor with integrated charges of (a) 0.05 C; (b) 0.1 C; (c) 0.2 C; and (d) 0.5 C. The insets show histograms of the length distribution of each sample; Gaussian fits to the data are displayed.

peroxide solution in the presence of zinc ions the following two reactions occur:



resulting in an overall deposition process of<sup>23,24</sup>



Reduction of hydrogen peroxide on the surface of the working electrode leads to the production of hydroxide ions and, hence, an increase in the local pH in the membrane channels. The increase of the local pH results in the formation of ZnO particles from zinc ions; that is, ZnO particles precipitate on the working electrode. ZnO nanorods develop because of the mass transport of zinc ions and hydrogen peroxide from bulk solution to the working electrode at the base of the membrane channels.

Field-emission scanning electron microscopy (FE-SEM) images of ZnO nanorods prepared at 22 °C by the electrochemical reduction of hydrogen peroxide, 5 mM, in the presence of zinc ions, 5 mM, at a track etched polymer membrane modified electrode are displayed in Figure 1. The diameter of the ZnO nanorods is  $100 \pm 20$  nm. Statistical analysis of the length distributions of the ZnO nanorods, inset in the FE-SEM images, yields the average lengths  $\langle l \rangle$  of 0.80, 1.45, 2.23, and 2.90  $\mu\text{m}$  for integrated charges of 0.01, 0.02, 0.05, and 0.1 C, respectively. The length dispersivity results from the intersection of membrane channels,<sup>1</sup> nonuniform pore size, and particle damage in centrifugation. The graph

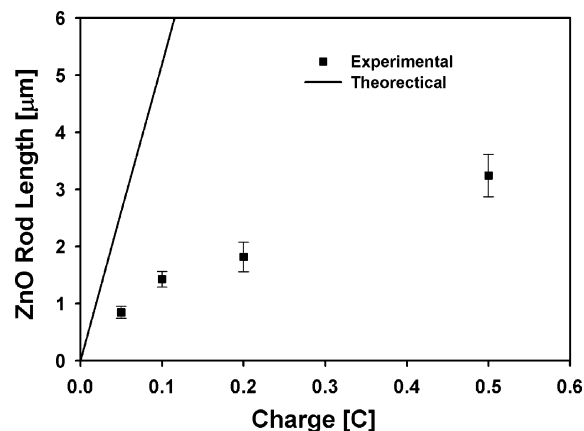


**Figure 5.** Experimental and theoretical (refer to Figure 2) relationships between the average length of ZnO nanorods prepared at 90 °C and the integrated charge passed during electrosynthesis. The vertical bars represent the full width at half-maximum of the Gaussian fit to the size histogram.

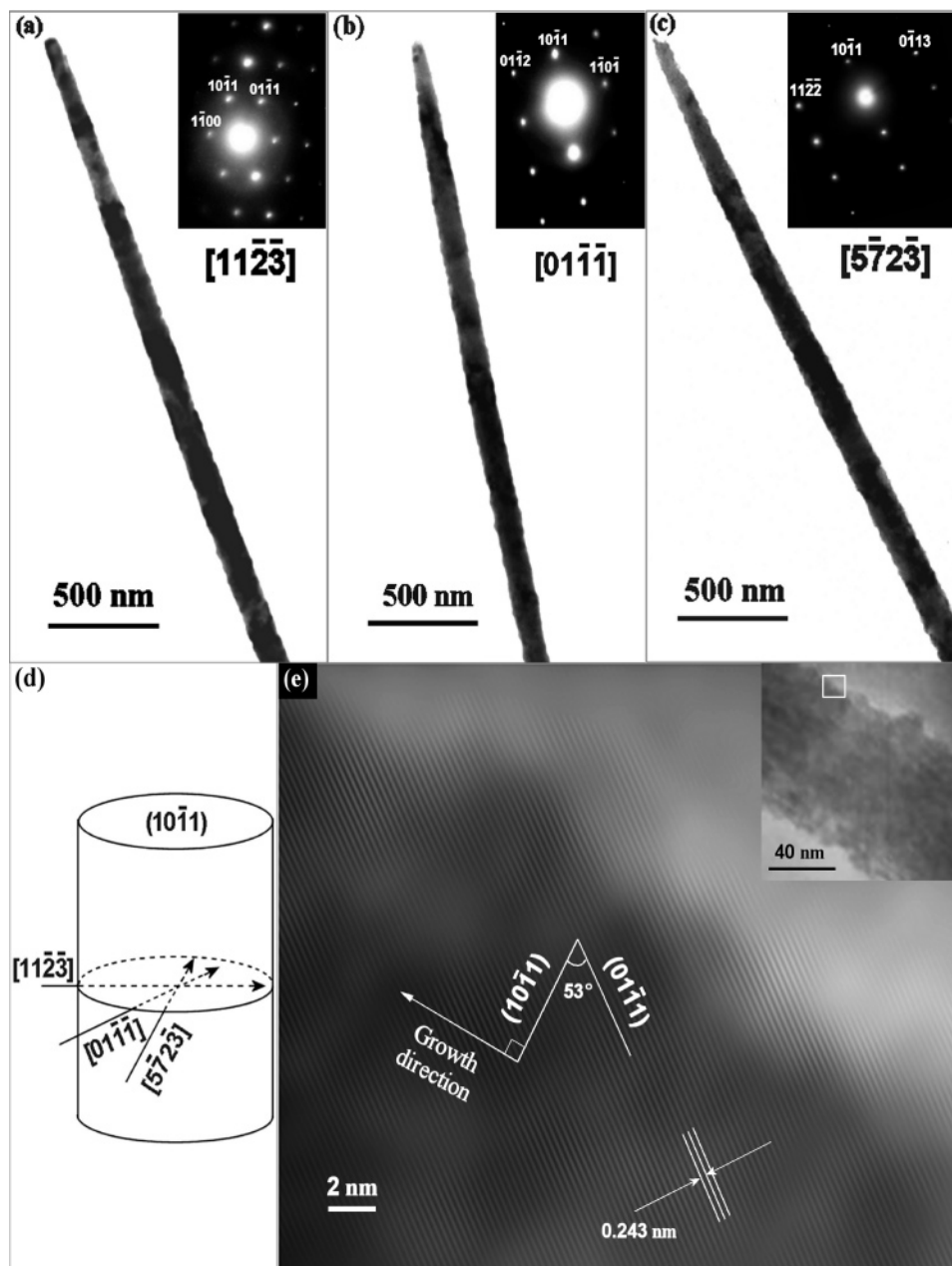
in Figure 2 demonstrates the relationship between  $\langle l \rangle$  and the integrated charge passed. The theory line shows the expected rod length if it is assumed that all electrons participate in reaction 3 and the rods have the same density as crystalline zinc oxide. In contrast to direct electrodeposition the length of the rods is not directly proportional to the charge passed because not all the hydrogen peroxide reduced forms ZnO. Nevertheless, the correlation indicates that the deposition charge can offer control of the length of ZnO nanorods formed.

Figure 3 shows a TEM image of ZnO nanorods grown at 22 °C in a solution containing hydrogen peroxide as the hydroxide precursor. The selected-area electron diffraction (SAED) pattern indicates that the as-prepared ZnO nanorods grown at this temperature are polycrystalline. To achieve greater crystallinity ZnO nanorods, higher preparation temperatures must be employed.

(23) Pauporté, T.; Lincot, D. *J. Electrochem. Soc.* **2001**, *148*, C310.

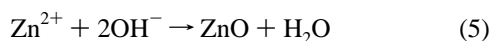
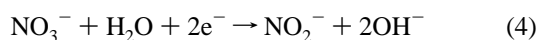
(24) Pauporté, T.; Lincot, D. *J. Electroanal. Chem.* **2001**, *517*, 54.



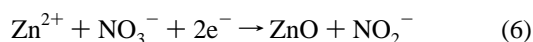


**Figure 6.** (a–c) TEM image of single ZnO nanorods and the corresponding SAED patterns along three zone axes; (d) configuration of the three electron beam directions for imaging the nanorods; and (e) HR-TEM image of a region of a ZnO nanorod (the region is indicated by the white box shown in the inset).

**2. Nitrate Ions as the Electrochemical Source of Hydroxide.** Rapid decomposition at high temperatures precludes the use of hydrogen peroxide at high temperatures. However, nitrate ions may be employed as an electrochemical hydroxide source at high temperatures. On the reduction of nitrate in the presence of zinc ions the following two reactions occur:



resulting in an overall deposition process of<sup>25,26</sup>



As in the case of hydrogen peroxide the mechanism involves,

first, an increase of pH, in this case due to the reduction of nitrate ions, and second the precipitation of zinc oxide. A FE-SEM image of the ZnO nanorods fabricated at 90 °C using nitrate ions as the electrochemical hydroxide precursor is shown in Figure 4. The diameter of the nanorods is in the range of  $120 \pm 40$  nm, a 20% increase in rod diameter for the higher reaction temperature. Statistical analysis of the length distributions of the ZnO nanorods, inset in the FE-SEM images, yields the average lengths  $\langle l \rangle$  of 0.85, 1.43, 1.82, and  $3.24 \mu\text{m}$  for integrated charges of 0.05, 0.1, 0.2, and 0.5 C, respectively. The graph in Figure 5 demonstrates the relationship between  $\langle l \rangle$  and the integrated charge passed. Further structural analysis was performed using TEM and HR-TEM. Three representative TEM images of single ZnO

(25) Izaki, M.; Omi, T. *Appl. Phys. Lett.* **1996**, *68*, 2439.

(26) Izaki, M.; Omi, T. *J. Electrochem. Soc.* **1996**, *143*, L53.

rods and the corresponding SAED patterns are displayed in Figure 6a–c. The diffraction patterns indicate that ZnO rods have a wurtzite structure. When recording the SAED patterns the incident beam was perpendicular to the nanorods. Thus, the fact that only the (10 $\bar{1}1$ ) is common to all three suggests that the ZnO growth direction is perpendicular to the (10 $\bar{1}1$ ) plane. Figure 6d displays the electron beam directions for imaging the nanorods along the [11 $\bar{2}3$ ], [01 $\bar{1}1$ ], and [5 $\bar{7}23$ ] zone axes, respectively. A HR-TEM image of a single ZnO rod is shown in Figure 6e. Identical planes were observed along the entire rod, that is, each rod displays characteristics of a single crystal. The measured plane spacing ( $\sim 0.243$  nm) is characteristic of the (01 $\bar{1}1$ ) planes of wurtzite zinc oxide. The measured angle ( $\sim 53^\circ$ ) between the (01 $\bar{1}1$ ) plane and the plane perpendicular to the growth direction is consistent with the literature value ( $52.19^\circ$ ) for the angle between (01 $\bar{1}1$ ) and (10 $\bar{1}1$ ), confirming that the growth direction of the ZnO nanorods is perpendicular to (10 $\bar{1}1$ ). It is of note that this growth direction differs from that normally observed for ZnO nanorods obtained by wet chemical methods. Despite the fact that the nonpolar surfaces exhibit lower energy<sup>27</sup> it is usual for ZnO rods to grow along the *c* axis with the crystal morphology dominated by the polar (0001) surface. It has been demonstrated<sup>27,28</sup> that in the initial stages of deposition thin layers of hexagonal Zn<sub>3</sub>O<sub>3</sub> rings are formed which favor

bulk deposition along the *c* axis. Film growth perpendicular to the (10 $\bar{1}1$ ) direction has been observed for ZnO growth on sodium chloride crystals; the alignment was rationalized in terms of epitaxy.<sup>29</sup>

### Conclusions

In summary, it has been shown that ZnO nanorods may be fabricated in porous polycarbonate membranes via an electrosynthesis route. The width of the nanorods is constrained by the uniform diameter of the membrane channels. The length of the polycrystalline rods grown at 22 °C can be controlled by the integrated charge passed during deposition. Single-crystal ZnO nanorods have been prepared at 90 °C using nitrate ions as hydroxide precursors. The growth direction of the ZnO rods grown at the higher temperature is perpendicular to the plane (10 $\bar{1}1$ ). It is anticipated that the methodology detailed above may be extended to a range of metal oxides.

**Acknowledgment.** M.L. would like to acknowledge Overseas Research Scholarship (ORS) scheme and the University of Bristol for financial assistance, and the authors thank Dr. S.A. Davis and Mr. J.A. Jones for their help in obtaining the HR-TEM images.

CM051613J

(27) Claeysens, F.; Freeman, C. L.; Allan, N. L.; Sun, Y.; Ashfold, M. N. R.; Harding, J. H. *J. Mater. Chem.* **2005**, *15*, 139.

(28) Hug, T.-B.; Hwang, Y.-H.; Kim H.-K.; Park, H.-L. *J. Appl. Phys.* **2004**, *96*, 1740.

(29) Henley, S. J.; Ashfold, M. N. R.; Cherns, D. *Thin Solid Films* **2002**, *422*, 69.